

Analytical expression of negative differential thermal resistance in a macroscopic heterojunction

Wataru Kobayashi*

Division of Physics, Faculty of Pure and Applied Sciences,
University of Tsukuba, Ibaraki 305-8571, Japan and

Tsukuba Research Center for Energy Materials Science (TREMS), University of Tsukuba, Ibaraki 305-8571, Japan

Heat flux (J) generally increases with temperature difference in a material. A differential coefficient of J against temperature (T) is called differential thermal conductance (k), and an inverse of k is differential thermal resistance (r). Although k and r are generally positive, they can be negative in a macroscopic heterojunction with positive T -dependent interfacial thermal resistance (ITR). The negative differential thermal resistance (NDTR) effect is an important effect that can realize thermal transistor, thermal memory, and thermal logic gate. In this paper, we examine analytical expressions of J , k , r , and other related quantities as a function of parameters related to thermal conductivity (κ) and ITR in a macroscopic heterojunction to precisely describe the NDTR effect.

I. INTRODUCTION

Thermal control is recently attracted much attention to address worldwide challenges such as energy harvesting, carbon neutral, warming temperatures, smart society, and sustainable development goals. The thermal-control technology consists of heat conduction, energy conversion, cooling, thermal storage, heat insulating, and thermal radiation technologies. Further, focusing on the heat conduction, thermal-circuit elements such as thermal rectifier, and thermal transistor, as a counterpart of electronic-circuit elements, are important to precisely control heat flux (J) [1, 2].

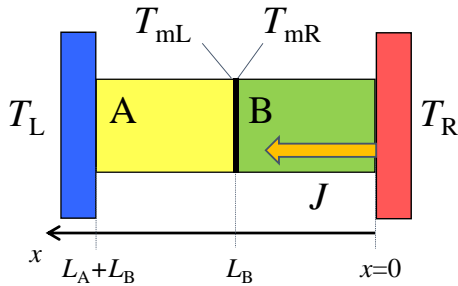


FIG. 1. (Color online) Schematic figure of a macroscopic heterojunction consists of juxtaposing material A and material B with interfacial thermal resistance (ITR) and non-uniform thermal conductivities (κ) against position (x) and temperature (T). The edge (at $x = 0$) of the material B is contacted with a heat bath with right-hand side (denoted by R) high temperature (T_R), and the heat flux (J) flows to a heat bath with left-hand side (L) low temperature (T_L) [$T_L < T_R$] at $x = L_A + L_B$ where an edge of the material A is contacted. At $x = L_B$, the materials A and B are connected, in which T -dependent ITR is introduced. The right(left)-hand side temperature at $x = L_B$ is denoted by $T_{mR}(T_{mL})$.

Thermal rectifier is an analogue of electrical rectifier, in which the heat flux in a forward direction is larger than that in the reverse direction. Theoretical calculations on the thermal rectification in microscopic one-dimensional system were reported [3–5]. In agreement with the theories, a thermal rectification in a carbon nanotube with mass gradient was demonstrated [6]. After that, a design of a bulk thermal rectifier was proposed [7]. In fact, the thermal rectification was demonstrated in bulk oxides [8]. Thus, both microscopic and macroscopic theories have successfully lead experimental realizations in both microscopic and macroscopic systems [1, 3, 4, 6–10].

Negative differential thermal resistance (NDTR) is a key effect which realizes thermal transistor [11, 12], thermal logic gate [13], and thermal memory [14]. In the thermal transistor, J can be amplified. An amplification factor (γ) defined by

$$\gamma \equiv \left| \frac{r_s}{r_s + r_d} \right|, \quad (1)$$

where r_s and r_d represent differential thermal resistances (r) at source and drain, respectively, becomes to be above one when r_s or r_d is negative [1, 11]. Thus, many theoretical efforts have been done to realize the NDTR effect. First, Li *et al.* investigated one-dimensional Frenkel-Kontorova (FK) lattice model and found NDTR effect [11]. Then, one dimensional atomic lattice models with mass gradient, two segment, different interactions, and/or on-site potentials were widely investigated and the NDTR effects were found by these theories [12, 15–19]. He *et al.* found that the origin of NDTR consists in the competition between temperature difference and a negative temperature dependence of thermal boundary conductance in a chain of two weakly coupled nonlinear lattices [15]. Shao *et al.* found that the NDTR effect highly depends on the properties of the interface and the system size in the two segment FK model [17]. Although NDTR effects were also found in graphene nanoribbons and heterojunction nanoribbons, as the length of the nanoribbons increases, unfortunately the NDTR effects gradually disappear [18, 19]. Thus, an experimental real-

* kobayashi.wataru.gf@u.tsukuba.ac.jp

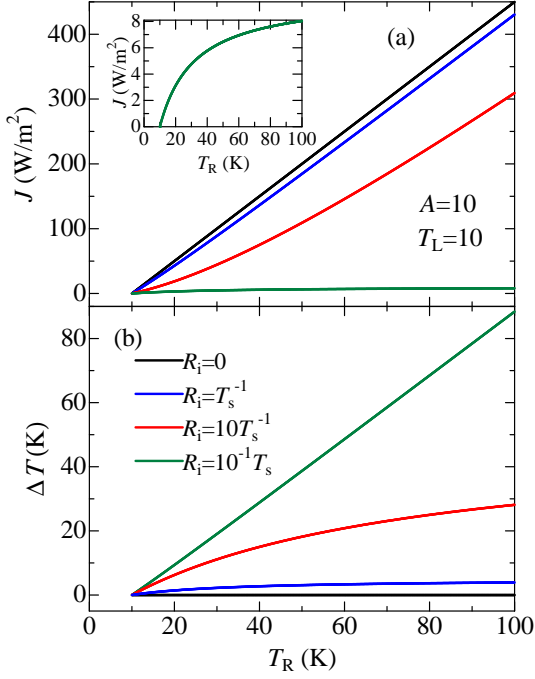


FIG. 2. (Color online) (a) Interfacial thermal resistance (R_i) dependence of J against right-hand side temperature (T_R) at high- T heat bath. A sum of T_{mL} and T_{mR} is defined as T_s [$T_s \equiv T_{mL} + T_{mR}$], where T_{mL} (T_{mR}) represents a left(right)-hand side temperature at the interface. (b) R_i dependence of temperature difference ($\Delta T \equiv T_{mR} - T_{mL}$) in between T_{mL} and T_{mR} at the interface against T_R . Lines in Figs. 2 (a) and (b) represent analytical expressions from Eqs. 11 and 12, respectively. Parameters A and T_L are fixed to be 10 and 10, respectively.

ization of the NDTR effect seems difficult to treat nano-scale objects with proper interfacial properties. Indeed, the NDTR effect has not been experimentally observed yet.

A bulk NDTR effect is promising for applicational points of view. Recently, Yang *et al.* theoretically found the bulk NDTR effect in a macroscopic homojunction with interface [20]. The NDTR element consists of juxtaposing bulk materials (materials A and B) with interface with interfacial thermal resistance (ITR) as shown in Fig. 1. When ITR exhibits a certain temperature dependence, the macroscopic homojunction present the bulk NDTR effect. Although they revealed the specific temperature dependence of ITR is essential to exhibit the bulk NDTR effect, they did not show precise analysis of this phenomenon.

In this paper, we investigate analytical expressions of the NDTR effect to understand the NDTR effect more precisely. J , k , r , and other related quantities are analytically described as a function of several parameters related to thermal conductivity (κ) and ITR in a macroscopic heterojunction.

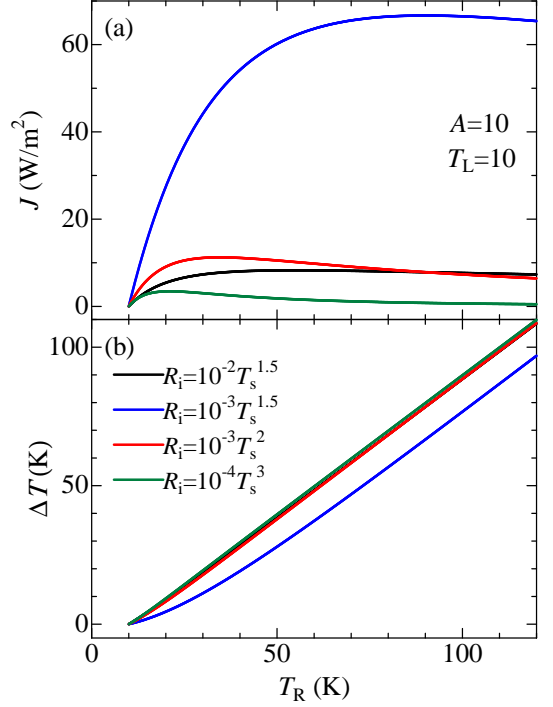


FIG. 3. (Color online) (a) R_i dependence of J against T_R . (b) R_i dependence of ΔT against T_R . Lines in Figs. 3 (a) and (b) represent analytical expressions from Eqs. 11 and 12, respectively. Parameters A and T_L are fixed to be 10 and 10, respectively.

II. METHODS

Fourier's law is a fundamental law for describing macroscopic heat conduction in condensed matter, which is derived from phenomenological equations [21]. In this paper, we assume insulated one-dimensional system consists of juxtaposing material A with the length of L_A and material B with the length of L_B with interface as shown in Fig. 1. The interface has temperature dependent interfacial thermal resistance (R_i). At the interface, temperature difference occurs due to R_i . A left(right)-hand side temperature at the interface is T_{mL} (T_{mR}) [m denotes middle]. Both the materials exhibit non-uniform thermal conductivity against x and $T(x)$. We use Fourier's law written as

$$J = -\kappa[x, T(x)] \frac{dT(x)}{dx}. \quad (2)$$

Since time derivative of internal energy density (u) is zero at steady state, $\nabla \cdot J = 0$ is obtained from the energy conservation law. Note that radiation loss is ignored in this paper. Thus, J becomes constant at any position in the one-dimensional system.

Then, integral of J with respect to x in the material B

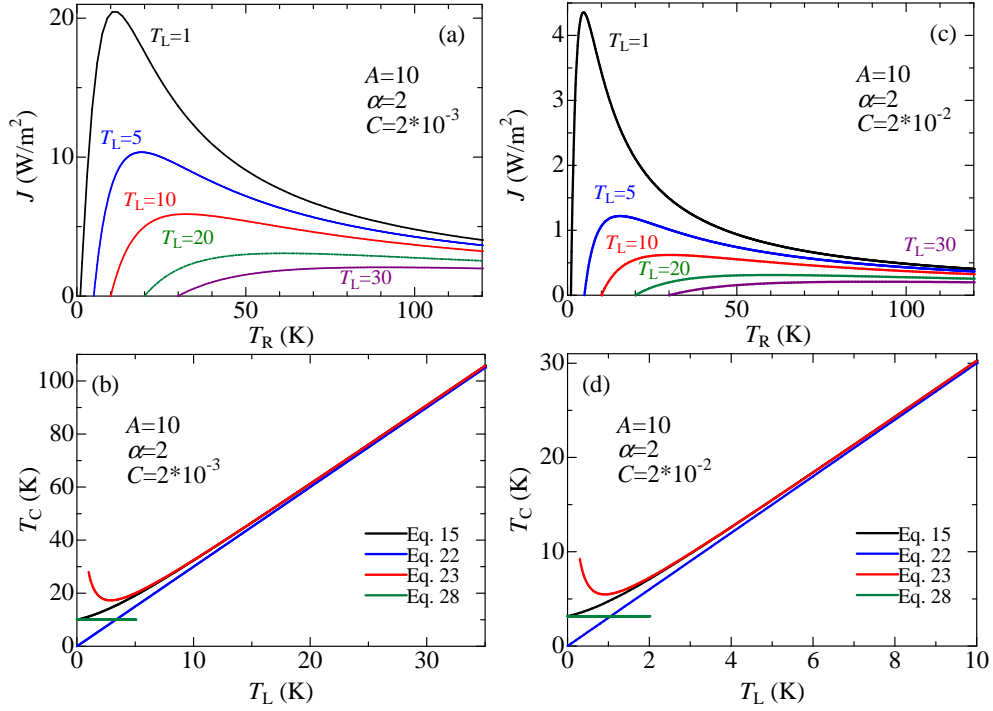


FIG. 4. (Color online) Parameter T_L dependence of J against T_R at (a) $A = 10$, $\alpha = 2$, and $C = 2 \times 10^{-3}$, (c) $A = 10$, $\alpha = 2$, and $C = 2 \times 10^{-2}$. A temperature (T_C) at $k \equiv \frac{\partial J}{\partial T_R} = 0$ against T_L described by analytical expressions Eqs. 15, 22, 23, and 28 at (b) $A = 10$, $\alpha = 2$, and $C = 2 \times 10^{-3}$, and at (d) $A = 10$, $\alpha = 2$, and $C = 2 \times 10^{-2}$.

is shown below,

$$\int_0^{L_B} J dx = \int_0^{L_B} -\kappa_B[x, T(x)] \frac{dT(x)}{dx} dx = \int_{T_{mR}}^{T_R} \kappa_B dT, \quad (3)$$

where κ_B , T_R , and T_{mR} represent, κ of the material B, a temperature at right-hand side high- T heat bath, and a right-hand side temperature at the interface ($x = L_B$), respectively. Similarly, the integral in the material A is shown below,

$$\begin{aligned} \int_{L_B}^{L_A+L_B} J dx &= \int_{L_B}^{L_A+L_B} -\kappa_A[x, T(x)] \frac{dT(x)}{dx} dx \\ &= \int_{T_L}^{T_{mL}} \kappa_A dT, \end{aligned} \quad (4)$$

where κ_A , T_L , and T_{mL} are κ of the material A, a temperature at left-hand side low- T heat bath, and a left-hand-side temperature at the interface, respectively.

Then, we introduce an interface with R_i . J at the interface is describes as

$$J = \frac{T_{mR} - T_{mL}}{R_i(T_{mL}, T_{mR})}. \quad (5)$$

Since J is constant at any position of x , Eq. 5 is equal

to Eqs. 3 and 4. Thus,

$$J = \frac{1}{L_A} \int_{T_L}^{T_{mL}} \kappa_A dT = \frac{T_{mR} - T_{mL}}{R_i(T_{mL}, T_{mR})} = \frac{1}{L_B} \int_{T_{mR}}^{T_R} \kappa_B dT \quad (6)$$

is obtained.

In this paper, as Yang *et al.* used [20], we assume power law as temperature dependence of ITR,

$$R_i(T_{mL}, T_{mR}) = C(T_{mR} + T_{mL})^\alpha, \quad (7)$$

where C is constant which regulates the magnitude of ITR, α is constant which regulates the power, and the sum $T_s \equiv T_{mR} + T_{mL}$ means mean temperature. As shown by Yang *et al.*, when $\alpha > 1$, the NDTR effect is occurred. This condition is easily derived by searching a condition that the T_{mR} derivative of J is zero ($\frac{\partial J}{\partial T_{mR}} = 0$) shown below,

$$T_{mR} = \frac{\alpha + 1}{\alpha - 1} T_{mL}. \quad (8)$$

$\alpha > 1$ is essential for positively reasonable solution $T_{mR} > T_{mL} > 0$.

To solve Eq. 6, here, both κ_A and κ_B are set to be constants as zeroth-order approximation. In addition, we set $\frac{\kappa_A}{L_A} = \frac{\kappa_B}{L_B} = A$. Then, two equations are derived

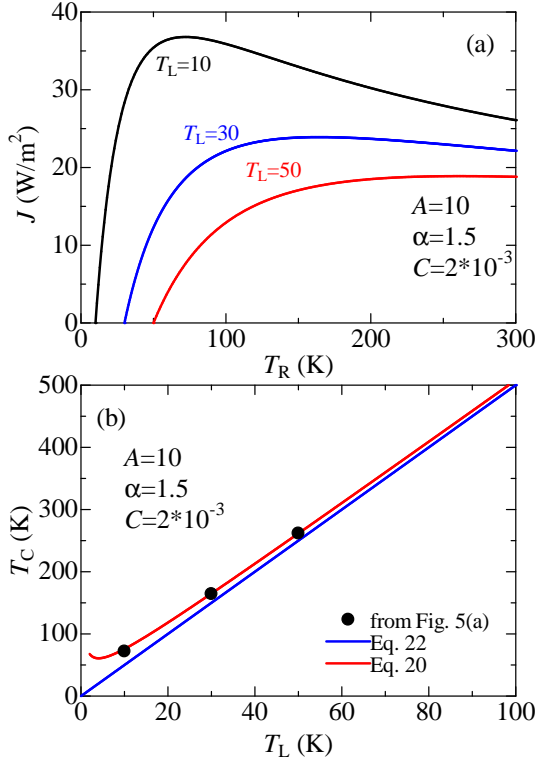


FIG. 5. (Color online) (a) T_L dependence of J against T_R at $A = 10$, $\alpha = 1.5$, and $C = 2 \times 10^{-3}$, and (b) T_c against T_L described by analytical expressions Eqs. 20, and 22 at $A = 10$, $\alpha = 1.5$, and $C = 2 \times 10^{-3}$. Dots are plotted from temperatures at $k = 0$ of the data in Fig. 5(a).

from Eq. 6 to obtain T_{mL} and T_{mR} as follows,

$$\begin{aligned} A(T_{mL} - T_L) &= A(T_R - T_{mR}), \\ \frac{T_{mR} - T_{mL}}{C(T_{mR} + T_{mL})^\alpha} &= A(T_R - T_{mR}). \end{aligned} \quad (9)$$

These polynomial equations can be analytically solved, and the both solutions of T_{mR} and T_{mL} are obtained. Then all the quantities T_{mR} , T_{mL} ($= T_R + T_L - T_{mR}$), J , ΔT , and k ($= r^{-1}$) are easily derived as a function of A , C , α , T_L , and T_R shown below,

$$T_{mR} = \frac{AC(T_R + T_L)^\alpha T_R + (T_R + T_L)}{2 + AC(T_R + T_L)^\alpha}, \quad (10)$$

$$J = A(T_R - T_{mR}) = \frac{A(T_R - T_L)}{2 + AC(T_R + T_L)^\alpha}, \quad (11)$$

$$\Delta T \equiv T_{mR} - T_{mL} = \frac{AC(T_R + T_L)^\alpha (T_R - T_L)}{2 + AC(T_R + T_L)^\alpha}, \quad (12)$$

$$\begin{aligned} k(= r^{-1}) &\equiv \frac{\partial J}{\partial T_R} \\ &= \frac{A}{2 + AC(T_R + T_L)^\alpha} \left(1 - \frac{\alpha \left(\frac{T_R - T_L}{T_R + T_L} \right)}{1 + \frac{2}{AC(T_R + T_L)^\alpha}} \right). \end{aligned} \quad (13)$$

Considering $J \geq 0$ and $\Delta T \geq 0$, $T_R \geq T_L$ is naturally derived. At $k = 0$, an equation is derived from Eq. 13 shown below,

$$AC(T_R + T_L)^{\alpha-1} \{(\alpha - 1)T_R - (\alpha + 1)T_L\} = 2 > 0. \quad (14)$$

Thus, a condition $(\alpha - 1)T_R - (\alpha + 1)T_L > 0$ must be realized, which leads $T_R > \frac{\alpha+1}{\alpha-1}T_L$ to observe NDTR. Eq. 14 can be analytically solved at $\alpha = 2$, and the solution is obtained as

$$T_c \equiv T_R(k = 0) = T_L + \sqrt{4T_L^2 + \frac{2}{AC}} > 3T_L. \quad (15)$$

Here, we assume $T_R = \frac{\alpha+1}{\alpha-1}T_L + \delta$. Then, Eq. 14 is simplified as

$$(\alpha - 1)AC\delta \left(\frac{2\alpha}{\alpha - 1}T_L + \delta \right)^{\alpha-1} = 2. \quad (16)$$

When $X \equiv \frac{2\alpha}{\alpha-1}T_L \gg \delta$ ($T_L \gg \frac{\alpha-1}{2\alpha}\delta$), the term $(\frac{2\alpha}{\alpha-1}T_L + \delta)^{\alpha-1}$ is expanded around $\delta = 0$ using Taylor expansion as,

$$\begin{aligned} (X + \delta)^{\alpha-1} &= X^{\alpha-1} + (\alpha - 1)X^{\alpha-2}\delta \\ &\quad + \frac{1}{2}(\alpha - 1)(\alpha - 2)X^{\alpha-3}\delta^2 + \dots \end{aligned} \quad (17)$$

Then, Eq. 16 becomes

$$(\alpha - 1)AC\delta \left(\frac{2\alpha}{\alpha - 1}T_L \right)^{\alpha-1} + \mathcal{O}(\delta^2) = 2. \quad (18)$$

Ignoring an order of δ^2 [$\mathcal{O}(\delta^2)$],

$$\delta \cong \frac{2}{(\alpha - 1)AC} \left(\frac{2\alpha}{\alpha - 1}T_L \right)^{1-\alpha}, \quad (19)$$

is obtained. Thus, T_c becomes

$$T_c \equiv T_R(k = 0) \cong \frac{\alpha + 1}{\alpha - 1}T_L + \frac{2}{(\alpha - 1)AC} \left(\frac{2\alpha}{\alpha - 1}T_L \right)^{1-\alpha}. \quad (20)$$

The condition $T_L \gg \frac{\alpha-1}{2\alpha}\delta$ becomes

$$T_L \gg \left(\frac{2}{(\alpha - 1)AC} \right)^{\frac{1}{\alpha}} \left(\frac{\alpha - 1}{2\alpha} \right), \quad (21)$$

by using Eq. 19. Thus, Eq. 20 becomes

$$\frac{T_c}{T_L} \cong \frac{\alpha + 1}{\alpha - 1} + \frac{2}{(\alpha - 1)AC} \left(\frac{2\alpha}{\alpha - 1}T_L \right)^{-\alpha} \rightarrow \frac{\alpha + 1}{\alpha - 1}, \quad (22)$$

when $T_L \gg \left(\frac{2}{(\alpha-1)AC}\right)^{\frac{1}{\alpha}} \left(\frac{\alpha-1}{2\alpha}\right)$. This result shows that low T_L and large α are necessary to realize low T_c . Eq. 15 becomes

$$T_c \cong 3T_L + \frac{1}{2ACT_L}, \quad (23)$$

when $T_L \gg \sqrt{\frac{1}{2AC}}$, which is equal to Eq. 20 at $\alpha = 2$.

Until now we saw analytical expressions of NDTR properties in the condition of Eq. 21. Next we would like to see analytical expressions of NDTR properties in a condition of $T_L \rightarrow 0$ limit, although $T_L = 0$ is unrealistic situation. Thus, we can have mathematically more simple analytical expressions and scaling behaviours, when $T_L = 0$ is substituted in Eqs. 10-13 as,

$$T_{mR0} = \frac{ACT_R^{\alpha+1} + T_R}{2 + ACT_R^{\alpha}}, \quad (24)$$

$$J_0 = A(T_R - T_{mR0}) = \frac{AT_R}{2 + ACT_R^{\alpha}}, \quad (25)$$

$$\Delta T_0 \equiv T_{mR0} - T_{mL0} = \frac{ACT_R^{\alpha+1}}{2 + ACT_R^{\alpha}}, \quad (26)$$

$$k_0 (= r_0^{-1}) \equiv \frac{\partial J_0}{\partial T_R} = \frac{A \left(1 - \frac{\alpha}{1 + ACT_R^{\alpha}}\right)}{2 + ACT_R^{\alpha}}, \quad (27)$$

where $T_{mL0} = T_R - T_{mR0}$. In addition, a temperature which exhibits the NDTR effect (T_{c0}) is analytically solved as,

$$T_{c0} = \left(\frac{2}{AC(\alpha-1)}\right)^{\frac{1}{\alpha}}, \quad (28)$$

when $T_L \rightarrow 0$.

Hu *et al.* previously have derived analytical expressions of NDTR with a different way from our method [22]. However, the expression is a formal solution, and is not specific. Compared with their work, our expressions are more specific, and easily compared with experiments.

III. RESULTS AND DISCUSSION

Figure 2(a) shows R_i dependence of J against T_R . At $R_i = 0$, J linearly increases. With non-zero R_i , magnitude of J decreases and the temperature dependence of J changes. The reduced magnitude is caused by increased magnitude of R_i . Figure 2(b) shows R_i dependence of ΔT in between T_{Lm} and T_{Rm} at a heterojunction against T_R . At $R_i = 0$, ΔT is zero against T_R , which is caused by absence of R_i . With non-zero R_i , magnitude of ΔT increases. The increased magnitude is caused by increased

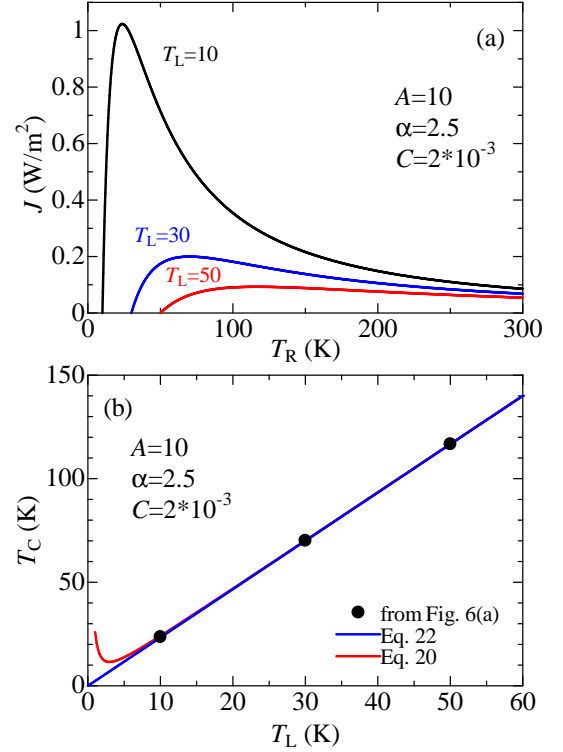


FIG. 6. (Color online) (a) T_L dependence of J against T_R at $A = 10$, $\alpha = 2.5$, and $C = 2 \times 10^{-3}$, and (b) T_c against T_L described by analytical expressions Eqs. 20, and 22 at $A = 10$, $\alpha = 2.5$, and $C = 2 \times 10^{-3}$. Dots are plotted from temperatures at $k = 0$ of the data in Fig. 6(a).

magnitude of R_i . All the magnitudes of J increases and NDTR is not observed below $\alpha = 1$, which is consistent with the theory.

Figure 3(a) shows R_i dependence of J against T_R . Above $\alpha = 1$, all the data of J shows reduction above T_c . Thus, the NDTR effect is observed. Figure 3(b) shows R_i dependence of ΔT against T_R . Above $\alpha = 1$, magnitude of ΔT also increases. The increased magnitude is caused by increased magnitude of R_i . The NDTR effect is observed above $\alpha = 1$, which is consistent with the theory.

Figure 4(a) shows T_L dependence of J against T_R at $A = 10$, $\alpha = 2$, and $C = 2 \times 10^{-3}$. With T_L , the magnitude of J decreases, and a temperature (T_c) which exhibits $k \equiv \frac{\partial J}{\partial T_R} = 0$ monotonically increases. The T_L dependent T_c is strictly understood as described in Method for $\alpha = 2$. Figure 4(b) shows T_c against T_L . The lines are analytical expressions of T_c from Eqs. 15, 22, 23, and 28 at $A = 10$, $\alpha = 2$, and $C = 2 \times 10^{-3}$. For $\alpha = 2$, T_L dependent T_c is strictly solved as Eq. 15. Eq. 15 is well approximated by Eq. 22 above ~ 20 K, and by Eq. 23 above ~ 5 K. At a limit of $T \rightarrow 0$, Eq. 15 becomes equal to Eq. 28. Substituting $C = 2 \times 10^{-2}$ for $C = 2 \times 10^{-3}$, figure 4 (c) depicts T_L dependence of J against T_R . Due to enhancement of R_i , the magnitude of J decreases com-

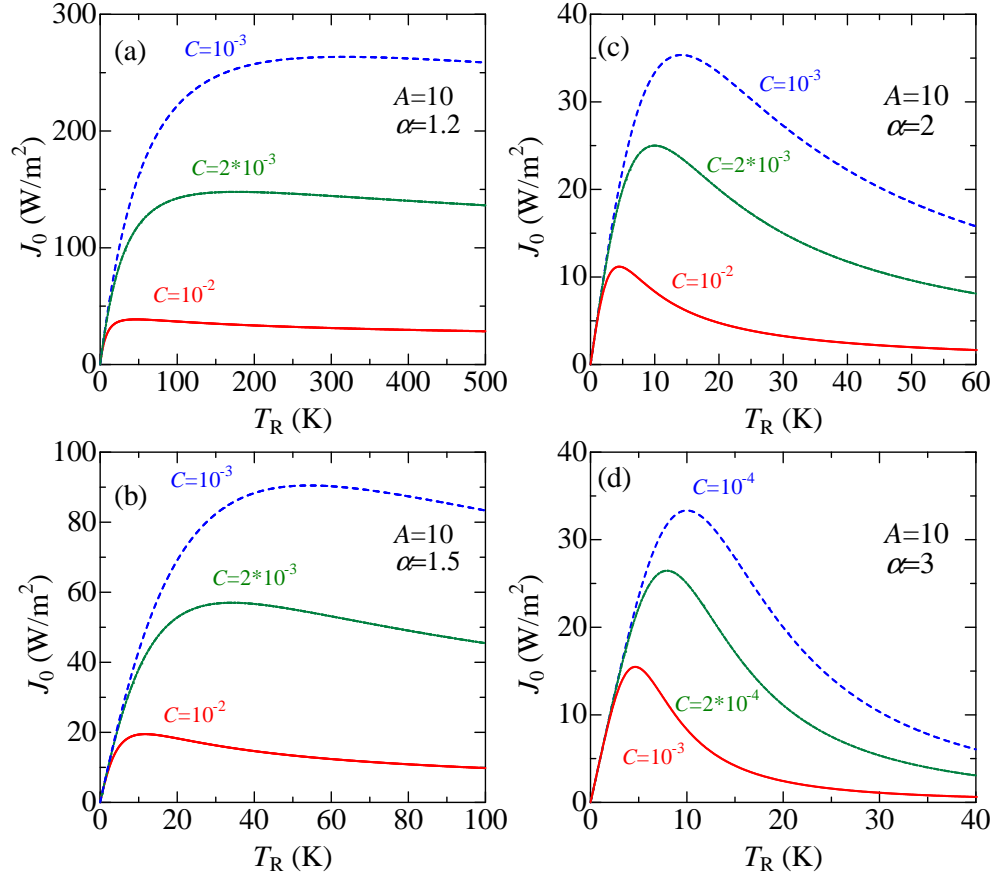


FIG. 7. (Color online) Parameter C dependence of J_0 against T_R at (a) $A = 10$ and $\alpha = 1.2$, (b) $A = 10$ and $\alpha = 1.5$, (c) $A = 10$ and $\alpha = 2$, and (d) $A = 10$ and $\alpha = 3$. All the lines represent analytical expressions from Eq. 25.

pared with that of J in fig. 4(a). As shown in Fig. 4(d), Eq. 15 is well approximated by Eq. 22 above ~ 6 K, and by Eq. 23 above ~ 2 K. The reductions of these temperatures compared with those in Fig. 4(b) are explained by Eq. 21.

Figure 5(a) shows T_L dependence of J against T_R at $A = 10$, $\alpha = 1.5$, and $C = 2 \times 10^{-3}$. With T_L , T_c monotonically increases. Figure 5(b) shows T_c against T_L from analytical expressions Eqs. 20, and 22 at $A = 10$, $\alpha = 1.5$, and $C = 2 \times 10^{-3}$. Dots are plotted from the T_c values of the data in Fig. 5(a). The dots are superimposed by Eq. 20.

Figure 6(a) shows T_L dependence of J against T_R at $A = 10$, $\alpha = 2.5$, and $C = 2 \times 10^{-3}$. With T_L , T_c monotonically increases. Figure 6(b) shows T_c against T_L from analytical expressions Eqs. 20, and 22 at $A = 10$, $\alpha = 2.5$, and $C = 2 \times 10^{-3}$. Dots are plotted from the T_c values of the data in Fig. 6(a). The dots are superimposed by both Eqs. 20 and 22. Thus, the NDTR behaviour at $T_R \gg 0$ is well understood. Namely, α is the most important parameter to determine T_c value at $T_L \gg 0$.

Next, we examine the NDTR behaviour at $T_L \rightarrow 0$, although $T_L = 0$ is unrealistic but mathematically in-

teresting. First, we check C and α dependences of J_0 . Figure 7 shows parameter C dependence of J_0 against T_R at (a) $A = 10$ and $\alpha = 1.2$, (b) $A = 10$ and $\alpha = 1.5$, (c) $A = 10$ and $\alpha = 2$, and (d) $A = 10$ and $\alpha = 3$. All the lines represent analytical expressions from Eq. 25. With C , all the magnitude of J_0 decreases, which is attributed to an increase of R_i . With α and C , T_{c0} monotonically decreases as shown in Eq. 28.

To further analyze these equations, we introduce dimensionless temperature $T' \equiv \frac{T_R}{T_{c0}}$, which shows scaling behavior. Substitution of $T_R = T' T_{c0}$ for Eq. 25 yields

$$J'_0 \equiv \frac{J_0}{AT_{c0}} = \frac{T'}{2 + \frac{2}{(\alpha-1)} T'^\alpha}. \quad (29)$$

Left-hand-side term represents dimensionless heat flux where AT_{c0} represents heat flux in the material at $T_R = T_{c0}$ and $T_L = 0$. The right-hand-side term is a function of dimensionless temperature T' and the power α . Thus, the temperature dependence of J'_0 is only dependent on α . In other words, the power α controls the temperature dependence of J'_0 . The dimensionless thermal conduc-

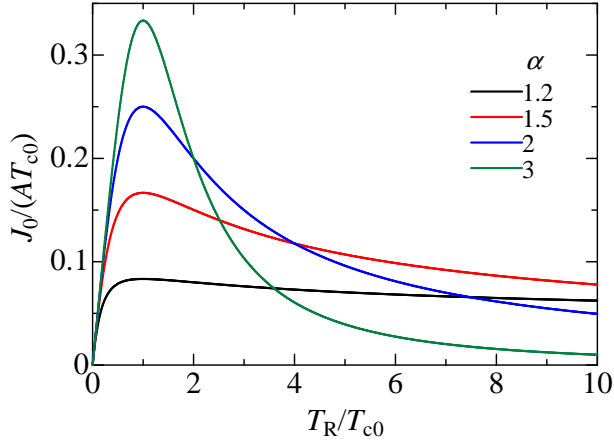


FIG. 8. (Color online) α dependence of dimensionless heat flux ($J'_0 \equiv \frac{J_0}{AT_{c0}}$) against dimensionless temperature ($T' \equiv \frac{T_R}{T_{c0}}$). All the lines represent analytical expressions from Eq. 29.

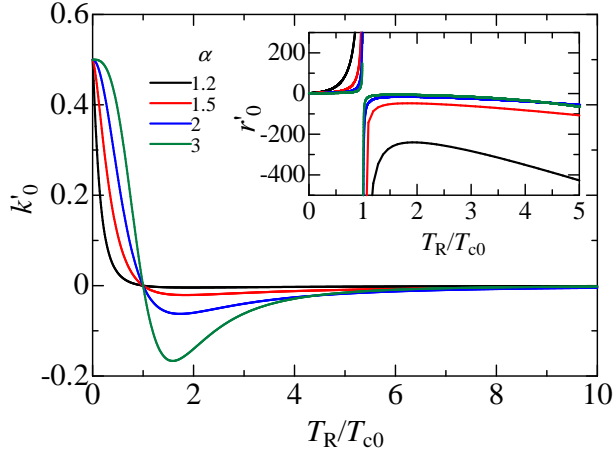


FIG. 9. (Color online) α dependence of dimensionless differential thermal conductance ($k'_0 \equiv \frac{\partial J'_0}{\partial T'}$) against T' . The inset shows dimensionless differential thermal resistance ($r'_0 \equiv k'_0{}^{-1}$) against T' . All the lines represent analytical expressions from Eq. 30.

tance $k'_0 (= r'_0{}^{-1}) \equiv \frac{\partial J'_0}{\partial T'}$ is easily derived as

$$k'_0 = \frac{1 - T'^\alpha}{2 \left(1 + \frac{1}{(\alpha-1)} T'^\alpha \right)^2}. \quad (30)$$

Figure 8 shows α dependence of dimensionless heat flux (J'_0) against dimensionless temperature (T'). All the lines represent analytical expressions from Eq. 29. With increasing α , peak structure at $T' = 1$ becomes sharper. Thus, α is the most important parameter in the model at $T_L = 0$.

Figure 9 shows α dependence of dimensionless differential thermal conductance (k'_0) against T' . All the lines

represent analytical expressions from Eq. 30. At a limit of $T_L \rightarrow 0$, all the magnitude of k is 0.5, which is represented by Eq. 30. Above $T' = 1$, the value of k'_0 becomes negative, and it merges to minus zero at a limit of $T_R = \infty$. The inset of figure 9 shows dimensionless differential thermal resistance ($r'_0 \equiv k'_0{}^{-1}$) against T' . All the lines represent analytical expressions from Eq. 30. Above $T' = 1$, the value of r'_0 becomes negative, and it diverges to $-\infty$ at a limit of $T_R = \infty$.

Lastly, we would like to comment on the temperature dependence of ITR. As we used in this paper, $\alpha > 1$ is essential to realize the NDTR effect. This means $R_i(T_{mL}, T_{mR})$ must increase with T . However, experimental results show that $R_i(T_{mL}, T_{mR})$ generally decreases with T [23]. As pointed out by Yang *et al.* [20], the NDTR effect can be realized using a material with negative thermal expansion due to thermal shrinkage characteristic to adjust the interface pressure. Indeed, Hohensee *et al.* have shown that R_i decreases with increasing pressure [24]. Thus, if one can adjust the shrinkage properly, negative pressure effect would be obtained. The negative pressure effect with T will enable the NDTR effect. There are many kinds of negative-thermal-expansion materials such as ZrW_2O_8 [25], rubber, siliceous faujasite [26], siliceous zeolites [27], and other inorganic materials [28]. Proper combinations of these materials and positive-thermal-expansion materials would yield such a interface with positively-temperature-dependent ITR. We saw analytical expressions of T_{mL} , T_{mR} , J , ΔT , T_c , k , r , and now understand how to control the NDTR effect in a macroscopic heterojunction at zeroth order approximation. In the model, we found that T_R dependence of J is analytically described using experimentally determinable parameters A , C , α , T_L , and T_R . We could also derive an analytical expression of T_c at the condition $T_L \gg 0$, which can control a temperature which exhibits NDTR behaviour. We also found that essentially only α controls temperature dependence of J_0 and k_0 at the limit of $T_L \rightarrow 0$. In other words, α is the most important parameter for all T_L value. Sharper peak structure of J (J_0) appears due to larger α . Thus, using technology of interface control, large α would be developed to realize experimentally detectable NDTR behaviour. We believe that this NDTR effect in a macroscopic heterojunction with positive temperature dependent ITR can be realized in near future.

IV. CONCLUSION

In conclusion, we examine analytical expressions of NDTR effect to reveal a condition that enables experimental realization of the NDTR effect. Using $\frac{\kappa_A}{L_A} = \frac{\kappa_B}{L_B} = A$ approximation as zeroth order approximation, T_{mL} , T_{mR} , J , ΔT , T_c , k , and r are analytically solved. All these NDTR parameters are described as a function of experimentally determinable parameters A , C , α , T_L , and T_R . In particular, at a limit of $T_L \rightarrow 0$, we found that

dimensionless heat flux ($J'_0 \equiv \frac{J_0}{AT_{c0}}$) is only dependent on α , in which larger α yields sharper peak structure of J . As shown in this work, $\alpha > 1$ is essential to realize the NDTR effect. This positive temperature dependence of R_i could be possible when one uses a material with neg-

ative thermal expansion to adjust the interface pressure.

V. ACKNOWLEDGMENT

We would like to thank H. Kobayashi and S. Kobayashi for support.

-
- [1] N. Li, J. Ren, L. Wang, G. Zhang, P. Hänggi, and B. Li, Colloquium: Phononics: Manipulating heat flow with electronic analogs and beyond, *Rev. Mod. Phys.* **84**, 1045 (2012).
 - [2] Y. Ding, G. Zhu, X. Shen, X. Bai, and B. Li, Advances of phononics in 2012-2022, *Chinese Phys. B* **31** 126301 (2022).
 - [3] M. Terraneo, M. Peyrard, and G. Casati, Controlling the energy flow in nonlinear lattices: A model for a thermal rectifier, *Phys. Rev. Lett.* **88**, 094302 (2002).
 - [4] B. Li, L. Wang and G. Casati, Thermal diode: rectification of heat flux, *Phys. Rev. Lett.* **93**, 184301 (2004).
 - [5] B. Li, J. Lan, and L. Wang, Interface thermal resistance between dissimilar anharmonic lattices, *Phys. Rev. Lett.* **95**, 104302 (2005).
 - [6] C. W. Chang, D. Okawa, A. Majumdar, and A. Zettl, Solid-state thermal rectifier, *Science* **314**, 1121 (2005).
 - [7] M. Peyrard, The design of a thermal rectifier, *Europhys. Lett.* **76**, 49 (2006).
 - [8] W. Kobayashi, Y. Teraoka, and I. Terasaki, An oxide thermal rectifier, *Appl. Phys. Lett.* **95**, 171905 (2009).
 - [9] N. Yang, G. Zhang, and B. Li, Thermal rectification in asymmetric graphene ribbons, *Appl. Phys. Lett.* **95**, 033107 (2009).
 - [10] D. Sawaki, W. Kobayashi, Y. Moritomo, I. Terasaki, Thermal rectification in bulk materials with asymmetric shape, *Appl. Phys. Lett.* **98**, 081915 (2011).
 - [11] B. Li, L. Wang, and G. Casati, Negative differential thermal resistance and thermal transistor, *Appl. Phys. Lett.* **88**, 143501 (2006).
 - [12] W. C. Lo, L. Wang, and B. Li, Thermal Transistor: Heat Flux Switching and Modulating, *J. Phys. Soc. Jpn.* **77**, 054402 (2008).
 - [13] L. Wang and B. Li, Thermal logic gates: computation with phonons, *Phys. Rev. Lett.* **99**, 177208 (2007).
 - [14] L. Wang and B. Li, Thermal memory: a storage of phononic information, *Phys. Rev. Lett.* **101**, 267203 (2008).
 - [15] D. He, S. Buyukdagli, and B. Hu, Origin of negative differential thermal resistance in a chain of two weakly coupled nonlinear lattices, *Phys. Rev. B* **80**, 104302 (2009).
 - [16] N. Yang, N. Li, L. Wang, and B. Li, Thermal rectification and negative differential thermal resistance in lattices with mass gradient, *Phys. Rev. B* **76**, 020301(R) (2007).
 - [17] Z.-G. Shao, L. Yang, H.-K. Chan, and B. Hu, Transition from the exhibition to the nonexhibition of negative differential thermal resistance in the two-segment Frenkel-Kontorova model, *Phys. Rev. E* **79**, 061119 (2009).
 - [18] J. Hu, Y. Wang, A. Vallabhaneni, X. Ruan, and Y. P. Chen, Nonlinear thermal transport and negative differential thermal conductance in graphene nanoribbons, *Appl. Phys. Lett.* **99**, 113101 (2011).
 - [19] X.-K. Chen, J. Liu, Z.-H. Peng, D. Du, and K.-Q. Chen, A wave-dominated heat transport mechanism for negative differential thermal resistance in graphene/hexagonal boron nitride heterostructures, *Appl. Phys. Lett.* **110**, 091907 (2017).
 - [20] Y. Yang, D. Ma, Y. Zhao, and L. Zhang, Negative differential thermal resistance effect in a macroscopic homojunction, *J. Appl. Phys.* **127**, 195301 (2020).
 - [21] L. Onsager, Reciprocal relations in irreversible process I, *Phys. Rev. B* **37**, 405 (1931).
 - [22] J. Hu, and Y. P. Chen, Existence of negative differential thermal conductance in one-dimensional diffusive thermal transport, *Phys. Rev. E* **87**, 062104 (2013).
 - [23] Y.-J. Wu, L. Fang and Y. Xu, Predicting interfacial thermal resistance by machine learning, *Npj Comput. Mater.* **5**, 56 (2019).
 - [24] G. T. Hohensee, R. B. Wilson, and D. G. Cahill, Thermal conductance of metal-diamond interfaces at high pressure, *Nat. Commun.* **6**, 6578 (2015).
 - [25] T. A. Mary, J. S. O. Evans, T. Vogt, and A. W. Sleight, Negative thermal expansion from 0.3 to 1050 kelvin in ZrW_2O_8 , *Science* **272**, 90 (1996).
 - [26] M. P. Attfield, and A. W. Sleight, Strong negative thermal expansion in siliceous faujasite, *Chem. Commun.* 601 (1998).
 - [27] P. Lightfoot, D. A. Woodcock, M. J. Maple, L. A. Villaescusa, and P. A. Wright, The widespread occurrence of negative thermal expansion in zeolites, *J. Mater. Chem.* **11**, 212 (2001).
 - [28] K. Takenaka, Negative thermal expansion materials: technological key for control of thermal expansion, *Sci. Technol. Adv. Mater.* **13**, 013001 (2012).